

Influence comparison of N_2 and NH_3 nitrogen sources on AlN films grown by halide vapor phase epitaxy

Jing-Jing Chen(陈晶晶), Jun Huang(黄俊), Xu-Jun Su(苏旭军), Mu-Tong Niu(牛牧童), Ke Xu(徐科)

Citation: Chin. Phys. B . 2020, 29(7): 076802 . **doi:** 10.1088/1674-1056/ab90ed
Journal homepage: http://cpb.iphy.ac.cn; http://iopscience.iop.org/cpb

What follows is a list of articles you may be interested in

Growth and aggregation of Cu nanocrystals on ionic liquid surfaces

Jia-Wei Shen(沈佳伟), Xun-Heng Ye(叶迅亨), Zhi-Long Bao(鲍志龙), Lu Li(李璐), Bo Yang(杨波), Xiang-Ming Tao(陶向明), Gao-Xiang Ye(叶高翔)

Chin. Phys. B . 2020, 29(6): 066801 . **doi:** 10.1088/1674-1056/ab8896

Effect of AlN coating on hydrogen permeability and surface structure of VT6 alloy by vacuum arc ion plating

Zi-Yi Ding(丁子祎)

Chin. Phys. B . 2019, 28(10): 108101 . **doi:** 10.1088/1674-1056/ab3a8e

Growth and transport properties of topological insulator Bi_2Se_3 thin film on a ferromagnetic insulating substrate

Shanna Zhu(朱珊娜), Gang Shi(史刚), Peng Zhao(赵鹏), Dechao Meng(孟德超), Genhao Liang(梁根豪), Xiaofang Zhai(翟晓芳), Yalin Lu(陆亚林), Yongqing Li(李永庆), Lan Chen(陈岚), Kehui Wu(吴克辉)

Chin. Phys. B . 2018, 27(7): 076801 . **doi:** 10.1088/1674-1056/27/7/076801

Generalized model for laser-induced surface structure in metallic glass

Lin-Mao Ye(叶林茂), Zhen-Wei Wu(武振伟), Kai-Xin Liu(刘凯欣), Xiu-Zhang Tang(汤秀章), Xiang-Ming Xiong (熊向明)

Chin. Phys. B . 2016, 25(6): 068104 . **doi:** 10.1088/1674-1056/25/6/068104

A review of the growth and structures of silicene on Ag (111)

Wu Ke-Hui

Chin. Phys. B . 2015, 24(8): 086802 . **doi:** 10.1088/1674-1056/24/8/086802

Influence comparison of N_2 and NH_3 nitrogen sources on AlN films grown by halide vapor phase epitaxy*

Jing-Jing Chen(陈晶晶)[1,2], Jun Huang(黄俊)[1], Xu-Jun Su(苏旭军)[1], Mu-Tong Niu(牛牧童)[1], and Ke Xu(徐科)[1,2,3,†]

[1] *Suzhou Institute of Nano-tech and Nano-bionics, Chinese Academy of Sciences, Suzhou* 215123, *China*
[2] *School of Physical Science and Technology, ShanghaiTech University, Shanghai* 201210, *China*
[3] *Suzhou Nanowin Science and Technology Co., Ltd., Suzhou* 215123, *China*

(Received 20 January 2020; revised manuscript received 9 April 2020; accepted manuscript online 7 May 2020)

A comparison of the nitrogen sources (N_2 and NH_3) influence on AlN films grown by high-temperature halide vapor phase epitaxy (HVPE) is reported. The x-ray rocking curves (XRCs) indicate that the full width at half maximum (FWHM) of (0002) plane for AlN films using N_2 as nitrogen source is generally smaller than that using NH_3. Optical microscope and atomic force microscope (AFM) results show that it is presently still more difficult to control the crack and surface morphology of AlN films with thicknesses of 5-10 μm using N_2 as the nitrogen source compared to that using NH_3. Compared with one-step growth, two-step growth strategy has been proved more effective in stress control and reducing the density of threading dislocations for AlN epilayers using N_2 as the nitrogen source. These investigations reveal that using N_2 as nitrogen source in HVPE growth of AlN is immature at present, but exhibits great potential.

Keywords: aluminum nitride, halide vapor phase epitaxy, surface structure, nitrogen source

PACS: 68.55.–a, 81.15.–z, 61.72.–y **DOI:** 10.1088/1674-1056/ab90ed

1. Introduction

The III-nitrides have attracted much attention owing to their wide range of band gap, high thermal conductivity, and high electrical resistivity. On account of the similar lattice constant and coefficient of thermal expansion with Al content AlGaN epilayer, AlN has become the irreplaceable substrate materials for solid and ultraviolet luminescence devices.[1] Currently, halide vapor phase epitaxy (HVPE) is one of the most promising methods to grow high quality AlN single crystals owing to its relatively high growth rate and ability to obtain high UV transparent films.[2] On the other hand, the nitrogen source ammonia, which is often used in the HVPE growth of AlN, will react with the chloride of Al to form various complexes. The pre-reaction between $AlCl_3$ and NH_3 before reaching the substrate consumes a large amount of Al source, decreasing the growth rate of AlN and deteriorating its surface.[3] To suppress the pre-reaction, many experiment researches and theoretical predictions of using N_2 as precursor gas in the metal-organic chemical vapor deposition (MOCVD) or plasma-enhanced atomic layer deposition (PEALD) growth of III-nitrides have been reported.[4–6] Our recent research[7] also found that using N_2 as nitrogen source in HVPE grown AlN could effectively inhibit the pre-reaction. The growth rate of AlN films grown by using N_2 increased linearly with the increase of the input ratio of N_2 and HCl flux (V/III ratio), rather than decreased exponentially in the growth by using NH_3 as the nitrogen source. This may be an assistant to illustrate that it is more advantageous to replace NH_3 with N_2 in HVPE growth of AlN.

Nevertheless, the low reactivity of N_2 at the conventional growth temperature of HVPE grown AlN introduced extra difficulties compared to the more mature growth process of using NH_3 as nitrogen source. In this paper, we present a comprehensive comparison research on the influence of nitrogen sources on AlN films grown by HVPE.

2. Experiments and measurements

The 2-in AlN films were grown on sapphire substrates with a miscut of about 1.5° toward the $[11\bar{2}0]$ axis at 1500 ℃ using a home-made high-temperature HVPE system.[8] $AlCl_3$ was generated by introducing HCl gas over the Al metal at 520 ℃ in the source zone of the reactor. Before growth, the sapphire substrates were initially heated to 1500 ℃ in a flowing NH_3 gas and then cleaned in H_2 at 1500 ℃ for 5 min. After the cleaning of the surface of the substrate, the input flux (N_2+H_2 or NH_3) rates were changed to the designed values for AlN growth. All samples were divided into four groups (A–D) depending on the nitrogen sources and the growth methods. Samples in groups A and B used N_2 as the nitrogen source, while samples in groups C and D used NH_3 as the nitrogen source. Among them, groups B and D were grown by a two-step method strategy. The detailed growth conditions of these films are listed in Table 1. The thicknesses of these samples were 5–10 μm. The quality of the AlN epilayers was examined

*Project supported by the National Key R&D Program of China (Grant No. 2017YFB0404100).
†Corresponding author. E-mail: kxu2006@sinano.ac.cn
© 2020 Chinese Physical Society and IOP Publishing Ltd

by x-ray diffraction (XRD, Bruker D8 Discover), optical microscope (Leica DM400M), atomic force microscope (AFM, NanoScope III tapping-mode), and transmission electron microscopy (200 kV FEI Talos F200X).

3. Results and discussion

The FWHMs of (0002)- and (10$\bar{1}$2)-plane x-ray rocking curves (XRCs) for the as-grown AlN films are shown in Fig. 1. The AlN epilayers grown by using N_2 and NH_3 as nitrogen sources are presented with red (N_2) and blue (NH_3) symbols, respectively. Among them, different shapes of markers distinguish one- and two-step growth methods. The FWHMs of the symmetric (0002) and skew-symmetric (10$\bar{1}$2) ω-scans are used to measure the tilt and twist mosaic of AlN,[9] respectively. It can be seen from Fig. 1(a) that the samples with FWHM of (0002) reflection smaller than 300 arcsec are AlN (N_2) films. The distribution of the FWHMs in Fig. 1(a) shows that the AlN (N_2) films can obtain smaller FWHM of (0002) reflection than the AlN (NH_3) films. In Fig. 1(b), the samples with FWHM of (10$\bar{1}$2) reflection below 500 arcsec are grown by the two-step method, and there is no significant difference for AlN (N_2) and AlN (NH_3) films. The XRD measurements reveal that using N_2 as nitrogen source in HVPE growth of AlN tends to obtain homogenous crystal orientation along the *c* axis. The two-step growth method seems more conducive to improving the crystal quality of AlN but also needs further evidence. According to the FWHMs of XRCs in Table 1, the dislocation densities of the as-grown AlN films are estimated. The results show that the samples with the lowest dislocation density among each group are A2, B1, C1, and D1, and the corresponding dislocation densities are 2.8×10^9 cm^{-2}, 1.9×10^9 cm^{-2}, 2.7×10^9 cm^{-2}, and 1.8×10^9 cm^{-2}, respectively.

To reveal the influence of N_2 and NH_3 nitrogen sources on the surface morphology of the HVPE grown AlN, films listed in Table 1 were prepared for a more intensive study. Optical micrographs (OMs) in Figs. 2 and 3 show the surface features of the as-grown AlN (N_2) and AlN (NH_3) films, respectively. The surfaces of the AlN (N_2) films grown by one-step method show a rough morphology on the macro scale. Many island structures that are several hundred micrometers in diameter appear on the surfaces. Nevertheless, the surfaces of the AlN (N_2) films grown by two-step method become smoother than the one-step films. The density and size of the islands appearing on the surfaces are greatly reduced. This indicates that an optimized two-step method is effective for the stress control on AlN (N_2) films. The surfaces of the AlN (NH_3) films in Fig. 3 are relatively smoother than the AlN (N_2) films, and have no large islands. The effect of the two-step method on improving the surfaces of the AlN (NH_3) films is not obvious, which is different from that of AlN (N_2) films.

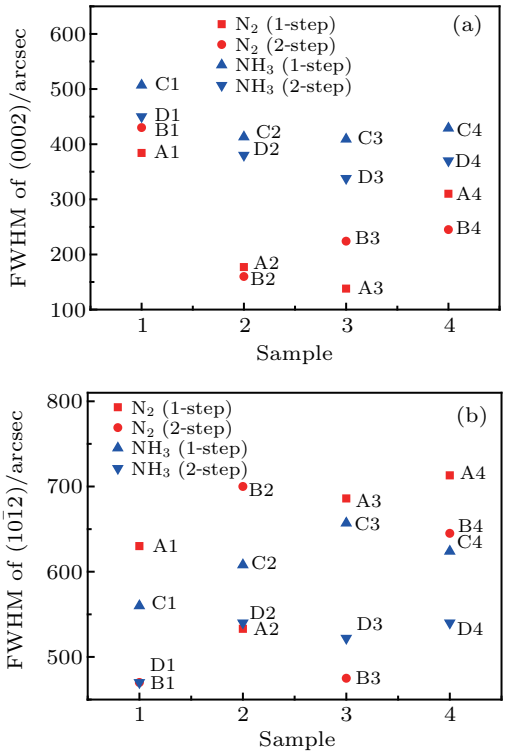


Fig. 1. The FWHMs of (0002) and (10$\bar{1}$2) plane XRCs for as-grown AlN films. The samples grown with different nitrogen sources are shown in different colors.

Table 1. The growth conditions and FWHM values of (0002)- and (10$\bar{1}$2)-plane XRCs for AlN epilayers.

Sample	HCl flux/sccm	N_2 flux/sccm	Input V/III	XRC FWHM/arcsec	
				(0002)	(10$\bar{1}$2)
A1	30	200	40	310	630
A2	20	300	90	384	533
A3	50	1000	120	177	686
A4	30	1000	200	138	713
B1	30	50	10	430	470
	50	20	2.4		
B2	10	1000	600	160	700
	50	1000	120		
B3	10	1000	600	224	475
	20	1000	300		
B4	10	1000	600	245	645
	30	1000	200		
C1	50	15	0.9	507	560
C2	50	50	3	413	608
C3	60	60	3	409	657
C4	30	40	4	429	624
D1	60	60	3	450	470
	50	30	1.8		
D2	60	60	3	380	540
	60	50	2.5		
D3	50	50	3	338	522
	60	60	3		
D4	30	100	10	370	540
	50	50	3		

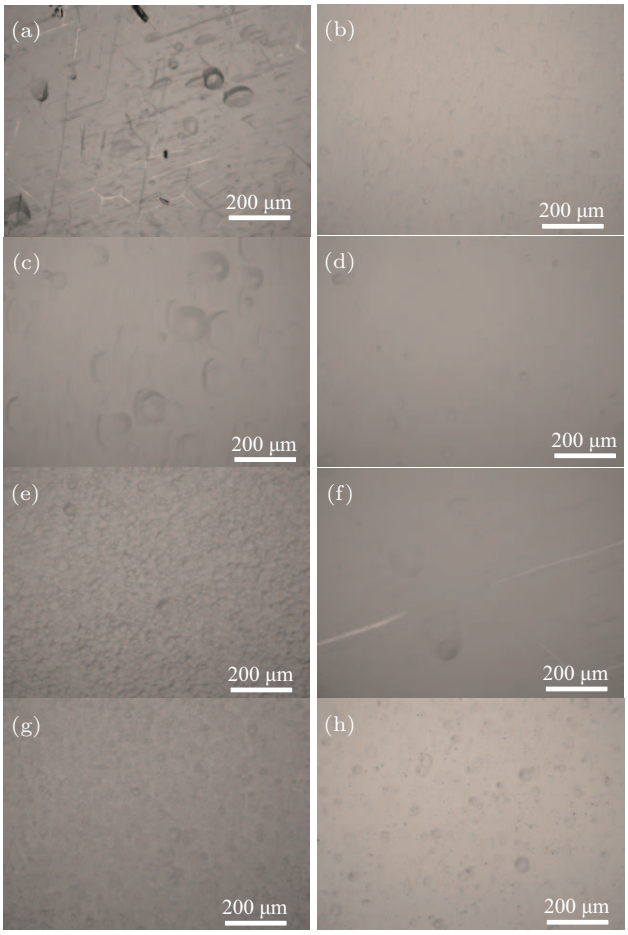


Fig. 2. Optical micrographs of AlN (N_2) samples: (a) A1, (c) A2, (e) A3, (g) A4; (b) B1, (d) B2,(f) B3, (h) B4.

Figure 4 shows the AFM images of four AlN samples that have the lowest dislocation density in each group as mentioned above. Among them, samples A2 and C1 were grown by one-step method, samples B1 and D1 were grown by two-step method. The normal directions of steps on both AlN epilayers are consistent with the off-cut direction of the sapphire substrates toward the [11$\bar{2}$0] axis. The difference is that, the steps on the AlN (N_2) films are undulating, while those on the AlN (NH_3) films are continuous and straight. The RMS roughness of the AlN (N_2) films is a little smaller than that of the AlN (NH_3) films for both one-step and two-step growth methods as shown in Fig. 4. Based on the results of optical microscopy and AFM measurements, it can be found that the two-step growth method can effectively improve the surface morphologies of the AlN (N_2) films. But it is still more difficult to control the surface morphologies of AlN (N_2) films than AlN (NH_3) films, due to the less mature growth technology for the former.

To further investigate the threading dislocations evolution in the AlN films, the cross-sectional TEM weak beam dark-field (WBDF) images of samples A2, B1, C1, and D1 were obtained with g vectors of 0002 and 11$\bar{2}$0, respectively. The vector of $g = 0002$ is commonly used to observe screw-component dislocations and inversion domains.[10] As can be seen in Fig. 5, the screw dislocations density of the AlN (N_2) films is smaller than that of the AlN (NH_3) films, which is consistent with the results of XRD. The vector of $g = 11\bar{2}0$ is used to identify the edge-component threading dislocations (TDs).[10] It can be found that both AlN films have a distinct edge dislocation merging process near the substrates. The most notable is that many edge (or mixed type) dislocations of sample B1 in Fig. 5(d) have a large angle of bending and then annihilate at about 1 μm above the substrate. It is speculated to be caused by the growth mode change during the two-step growth process.[11,12] When the V/III ratio is high at the first growth step, the vertical growth rate is higher than the lateral growth rate.[13] Then, large islands will form on the surface. When the V/III ratio becomes lower at the second growth step, the lateral growth will be dominant.[13] Ultimately, the mirror force caused by the merging of islands drives the dislocations bending. However, this annihilation mechanism of dislocations is not obvious in the two-step grown AlN (NH_3) film as shown in Fig. 5(h).

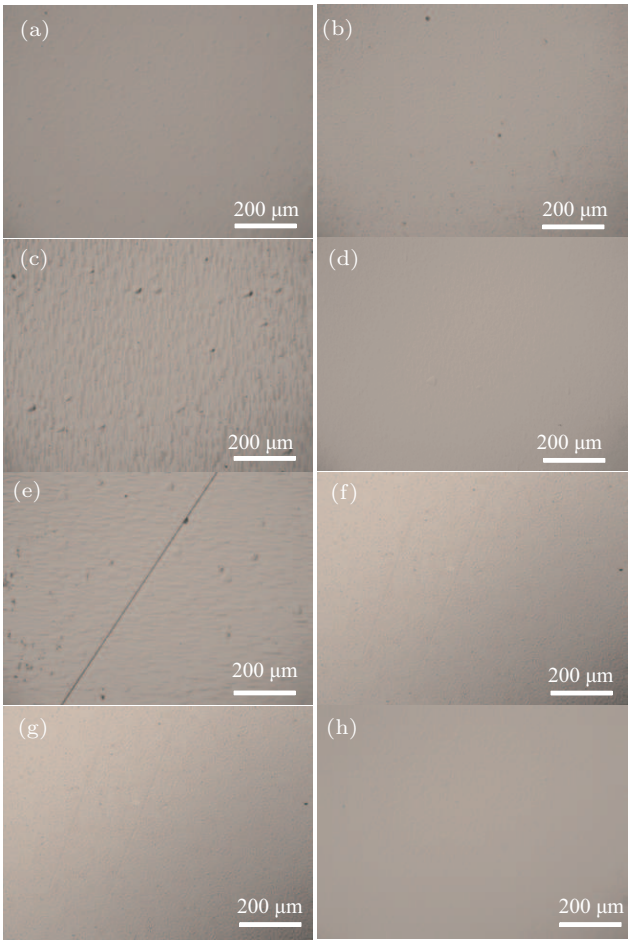


Fig. 3. Optical micrographs of AlN (NH_3) samples: (a) C1, (c) C2, (e) C3, (g) C4; (b) D1, (d) D2,(f) D3, (h) D4.

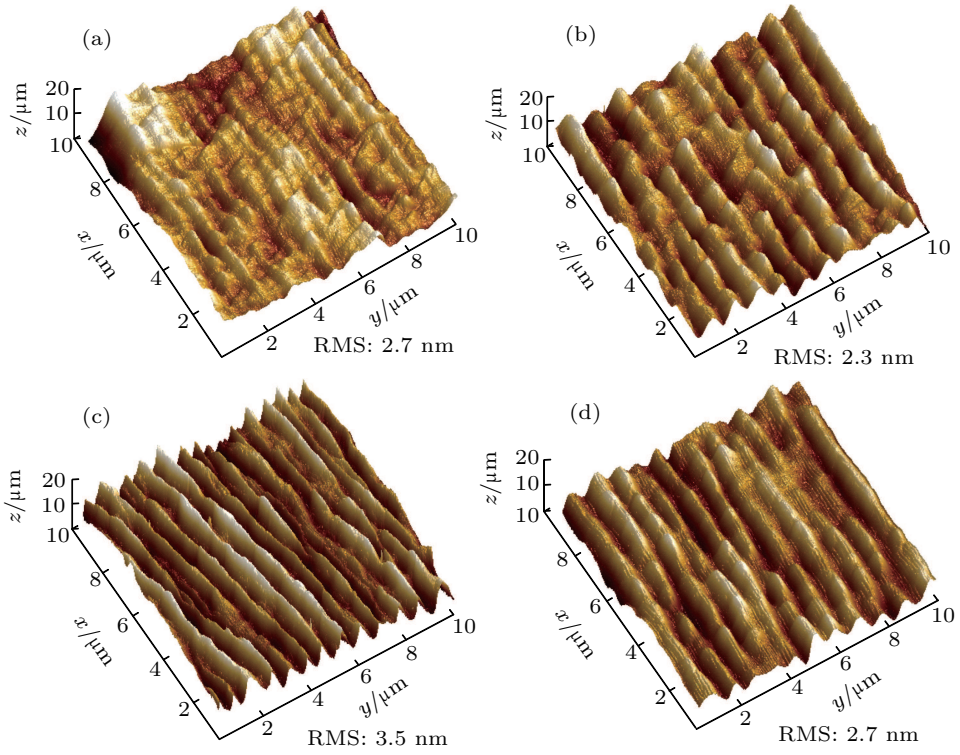


Fig. 4. The 10 μm×10 μm AFM images of the as-grown AlN samples: (a) A2, (b) B1, (c) C1, and (d) D1.

It is also found that a high density of columnar inversion domains (IDs) (indicated by white arrows in Figs. 5(a) and 5(c)) formed above the substrates in all AlN films. The origin of these IDs in AlN was reported to be related to the decomposition of the sapphire substrate.[14] These inversion domains were determined by the comparison of the contrast between the V-shaped columns and the surrounding matrix when switching from $g = 0002$ and $g = 000\bar{2}$ in non-centrosymmetric axis $[11\bar{2}0]$.[14–16] Since the columnar inversion domains in our experiment all formed close structures and did not extend to the surface, the overall polarity of the films was not influenced by them. The circles in Fig. 5(c) point out several V-shaped structures composed by inversion domains. These locations correspond exactly to the region with the lowest density of dislocation in Fig. 5(d). We speculate that the process of the island merging in sample B1 may affect the distribution of the inversion domains. The specific relationship between the inversion domains and island merging is difficult to determine from the present experimental results, and further investigations are needed.

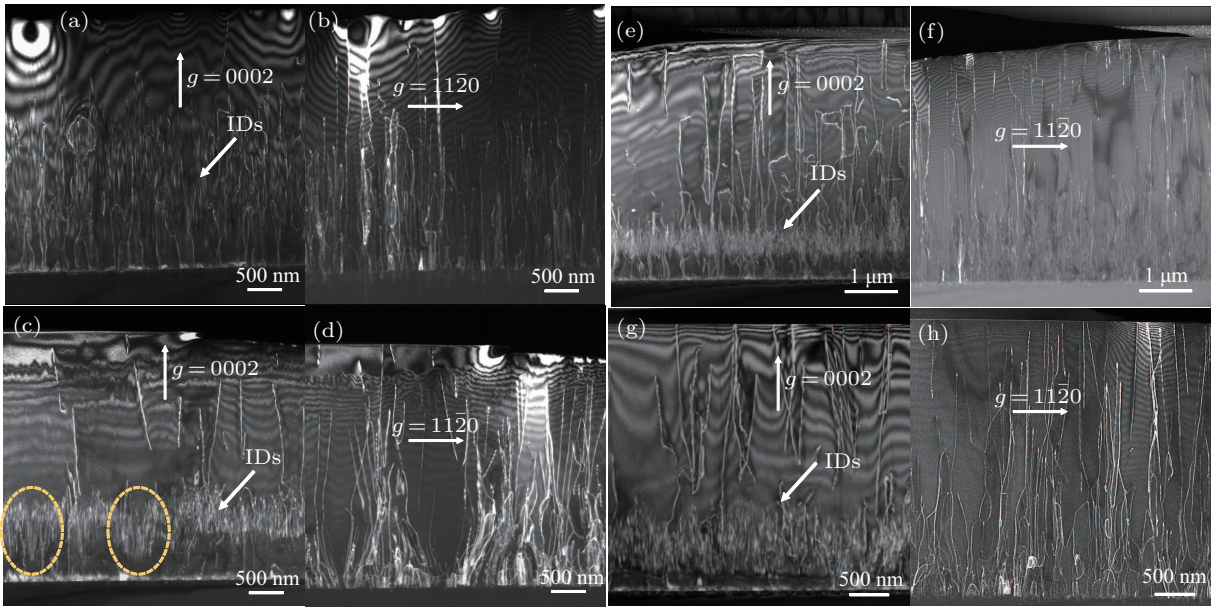


Fig. 5. TEM weak beam dark-field images of samples (a), (b) A2, (c), (d) B1, (e), (f) C1, and (g), (h) D1. Each sample was recorded with g vectors of 0002 and $11\bar{2}0$, respectively. The white arrows in (a) indicate the location of inversion domains.

4. Conclusion

The influence of N_2 and NH_3 nitrogen sources on the crystal quality and surface morphology of AlN films grown by HVPE has been comprehensively investigated. In most cases, AlN films grown using N_2 nitrogen sources have smaller FWHMs of (0002) plane XRCs than those grown using NH_3 nitrogen sources, while having no significant difference for the FWHMs of $(10\bar{1}2)$ plane XRCs. An optimized two-step method can improve the surface morphology and reduce the dislocation density of AlN films, and it is especially effective for the AlN films grown using N_2 as the nitrogen source. At present, it is still more difficult to control the crack and surface morphology of AlN films with thicknesses of 5–10 μm grown using N_2 as nitrogen source compared to that grown using NH_3, due to the less mature growth technology for the former.

References

[1] Kaeding J F, Wu Y, Fujii T, Sharma R, Fini P T, Speck J S and Nakamura S 2004 *J. Cryst. Growth* **272** 257

[2] Huang C Y, Wu P Y, Chang K S, Lin Y H, Peng W C, Chang Y Y, Li J P, Yen H W, Wu Y S, Miyake H and Kuo H C 2017 *AIP Adv.* **7** 055110

[3] Timoshkin A Y, Bettinger H F and Schaefer H F 1997 *J. Am. Chem. Soc.* **119** 5668

[4] Alevli M, Ozgit C, Donmez I and Biyikli N 2011 *J. Cryst. Growth* **335** 51

[5] Danielsson Ö and Janzén E 2003 *J. Cryst. Growth* **253** 26

[6] Shen X Q, Kojima K, Shimizu M and Okumura H 2018 *Crystengcomm* **20** 7364

[7] Huang J, Chen Q J, Niu M T and Xu K 2020 *J. Cryst. Growth* **536** 125567

[8] Huang J, Niu M T, Zhang J C, Wang W, wang J F and Xu K 2017 *J. Cryst. Growth* **459** 159

[9] Liu J Q, Wang J F, Liu Y F, Huang K, Hu X J, Zhang Y M, Xu Y, Xu K and Yang H 2009 *J. Cryst. Growth* **311** 3080

[10] Wu X H, Brown L M, Kapolnek D, Keller S, Keller B, DenBaars S P and Speck J S 1996 *J. Appl. Phys.* **80** 3228

[11] Imura M, Fujimoto N, Okada N, Balakrishnan K, Iwaya M, Kamiyama S, Amano H, Akasaki I, Noro T, Takagi T and Bandoh A 2007 *J. Cryst. Growth* **300** 136

[12] Ji Z S, Wang L S, Zhao G J, Meng Y L, Li F Z, Li H J, Yang S Y and Wang Z G 2017 *Chin. Phys. B* **26** 078102

[13] Kitagawa S, Miyake H and Hiramatsu K 2014 *Jpn. J. Appl. Phys.* **53** 05FL03

[14] Su X, Zhang J, Huang J, Zhang J, Wang J and Xu K 2017 *J. Cryst. Growth* **467** 82

[15] Romano L T, Northrup J E and OKeefe M A 1996 *Appl. Phys. Lett.* **69** 2394

[16] Stolyarchuk N, Markurt T, Courville A, March K, Zúñiga-Pérez J, Vennéguès P and Albrecht M 2018 *Sci. Rep.* **8** 14111